THE JOURNAL OF BIOLOGICAL CHEMISTRY VOL. 286, NO. 4, pp. 3018–3032, January 28, 2011
© 2011 by The American Society for Biochemistry and Molecular Biology, Inc. Printed in the U.S.A.

Biochemical and Morphological Properties of Hepatitis C Virus Particles and Determination of Their Lipidome*[S]

Received for publication, August 13, and in revised form, November 3, 2010 Published, JBC Papers in Press, November 5, 2010, DOI 10.1074/jbc.M110.175018

Andreas Merz[‡1,2], Gang Long[‡1,2,3], Marie-Sophie Hiet[‡3], Britta Brügger[§4], Petr Chlanda[¶], Patrice Andre[‖], Felix Wieland[§4], Jacomine Krijnse-Locker[‡], and Ralf Bartenschlager[‡5]

From the [‡]Department of Infectious Diseases, Molecular Virology, University of Heidelberg, Im Neuenheimer Feld 345, 69120 Heidelberg, Germany, the [§]Heidelberg University Biochemistry Center, University of Heidelberg, Im Neuenheimer Feld 328, 69120 Heidelberg, Germany, the [¶]Structural/Computational Biology Programme, EMBL Heidelberg, Meyerhofstrasse 1, 69117 Heidelberg, Germany, and [‖]INSERM U851, University of Lyon, 21 Avenue Tony Garnier, 69365 Lyon Cedex 07, France

A hallmark of hepatitis C virus (HCV) particles is their association with host cell lipids, most notably lipoprotein components. It is thought that this property accounts for the low density of virus particles and their large heterogeneity. However, the composition of infectious virions and their biochemical and morphological properties are largely unknown. We developed a system in which the envelope glycoprotein E2 was N-terminally tagged with a FLAG epitope. This virus, designated Jc1E2^{FLAG}, produced infectivity titers to wild type levels and allowed affinity purification of virus particles that were analyzed for their protein and lipid composition. By using mass spectrometry, we found the lipid composition of Jc1E2^{FLAG} particles to resemble the one very low- and low density-lipoprotein with cholesteryl esters accounting for almost half of the total HCV lipids. Thus, HCV particles possess a unique lipid composition that is very distinct from all other viruses analyzed so far and from the human liver cells in which HCV was produced. By electron microscopy (EM), we found purified Jc1E2^{FLAG} particles to be heterogeneous, mostly spherical structures, with an average diameter of about 73 nm. Importantly, the majority of E2-containing particles also contained apoE on their surface as assessed by immuno-EM. Taken together, we describe a rapid and efficient system for the production of large quantities of affinity-purified HCV allowing a comprehensive analysis of the infectious virion, including the determination of its lipid composition.

Chronic infection with the hepatitis C virus (HCV)[6] is among the most frequent cause of liver cirrhosis and hepatocellular carcinoma (1). About 3% of the world population is thought to be chronically infected with HCV, and these people have a high risk to develop serious liver diseases. As approved selective drugs are not available, chronic hepatitis C is treated with a combination of pegylated interferon-α and ribavirin. However, cure rates are not satisfactory, and treatment is associated with numerous side effects.

HCV has been classified as the separate genus *Hepacivirus* in the family Flaviviridae to which the genera *Pestivirus* and *Flavivirus* belong. Viruses of this family possess a positive-strand RNA genome that in case of HCV is 9.6 kb long and encodes for a single polyprotein of ~3,000 amino acids. It is cleaved co and post-translationally by cellular and viral proteases into 10 different products (2). The N-terminally residing structural protein cores, envelope protein 1 (E1) and envelope protein 2 (E2), are thought to be the major constituents of infectious HCV particles. C-terminally of E2 resides p7, a small protein that forms oligomeric complexes acting as viroporin (3), and nonstructural protein 2 (NS2) that, together with p7, contributes to virus assembly (4–6). The other viral proteins NS3, NS4A, NS4B, NS5A, and NS5B most likely form the core of the HCV replicase that catalyzes the amplification of the viral RNA genome (2).

Although our knowledge about structure and (enzymatic) activities of viral proteins has increased tremendously (7), the biochemical and morphological features of HCV particles still remain elusive. This is mainly due to low virus titers in infected tissues and, until recently, the lack of culture systems producing sufficient amounts of infectious HCV particles. This hurdle has been overcome by the identification of a particular genotype 2a HCV isolate (designated JFH1) that replicates to very high levels in cell culture and supports infectious particle production (8, 9). Moreover, highly efficient JFH1-derived chimeras have been generated. In some of them, the region encoding the JFH1 core to NS2 has been replaced by the corresponding region of other HCV isolates (10–12). Most efficient is the intragenotypic chimera Jc1 supporting virus titers in the range of 10^6 infectious units per ml, which is ~1,000-fold higher as compared with JFH1 (12).

Up to now, characterization of HCV particles is based on studies using partially purified virions from patient sera, experimentally inoculated chimpanzees, or rather low titer JFH1 particle preparations generated in cell cultures (9, 13–17). It is well established that infectious HCV particles have a low den-

* This work was supported in part by the Deutsche Forschungsgemeinschaft Sonderforschungsbereich 638, Teilprojekt A5 (to R. B.).
[S] The on-line version of this article (available at http://www.jbc.org) contains supplemental Figs. S1–S5, Tables S1 and S2, and additional references.
[1] Both authors contributed equally to this work.
[2] Supported in part by European Research Council Grant 233130.
[3] Supported by a grant from the European Union (Marie Curie Training Network EI-HCV, Contract MRTN-CT-2006-035599 EI-HCV).
[4] Supported by Grant SFB TRR83 from the Deutsche Forschungsgemeinschaft.
[5] To whom correspondence should be addressed. Tel.: 49-6221-56-4569; Fax: 49-6221-56-4570; E-mail: ralf_bartenschlager@med.uni-heidelberg.de.
[6] The abbreviations used are: HCV, hepatitis C virus; apo, apolipoprotein; Cer, ceramide; CypA, cyclophilin A; DENV, Dengue virus; HexCer, hexosylceramide; PE, phosphatidylethanolamine; PG, phosphatidylglycerol; PI, phosphatidylinositol; PS, phosphatidylserine; SM, sphingomyelin; SR-BI, scavenger receptor BI; TAG, triacylglycerol; qRT, quantitative RT.

sity (≤1.1 g/ml) that appears to be determined by the host cell, in which the virus is produced (18). This is probably due to the tight association of virions with host cell components, most notably lipoproteins (15, 16, 19). The association appears to occur during assembly, because HCV formation and secretion depend on components of the very low density lipoprotein (VLDL) assembly and secretion pathways, including apolipoprotein E (apoE) and microsomal triglyceride transfer protein (19–23). Whether apolipoprotein B (apoB) is also required for HCV assembly is discussed controversially (19, 21, 22, 24). ApoB-containing lipo-viro-particles have been identified in patients (16). Moreover, expression of the HCV envelope glycoproteins in the human small intestinal cell line CaCo2 gives rise to apoB-48 containing E1/E2-positive triglyceride-rich lipoprotein particles arguing for an intrinsic association of HCV envelope proteins with this apolipoprotein. However, Huh7 and Huh7.5 cells have proven deficient for this association, although they secrete apoB (25).

Apart from its role in HCV particle morphogenesis, apoE seems to enhance HCV entry by interacting with low density lipoprotein receptor (26). Likewise, apoB-containing lipoproteins (27) or high density lipoprotein (HDL) (28) appear to facilitate the interaction of HCV pseudoparticles or cell culture-grown HCV with scavenger receptor class B type I (SR-BI) (29). The exchangeable apolipoprotein apoCI, which is predominantly present in HDL, seems to interact with HCV particles via hypervariable region 1 (HVR1) in the N terminus of E2 thus promoting interaction and fusion of the HCV envelope with cellular membranes (30, 31).

Assembly of VLDL starts with the cotranslational lipidation of apoB-100 by microsomal triglyceride transfer protein delivering lipids from cytosolic lipid droplets into the endoplasmic reticulum lumen (32, 33). The resulting primordial lipoprotein is further lipidated into a triglyceride-poor form of VLDL that is released from the endoplasmic reticulum at distinct exit sites and transported to the Golgi apparatus. From there it can be secreted as such or is lipidated into a large triglyceride-rich form of VLDL, depending on triglyceride levels. Interestingly, apoE seems to be a key factor for the bulk addition of lipids to VLDL by regulating fusion with luminal lipid droplets in a distal compartment of the secretory pathway (reviewed in Ref. 34). *In vivo* hepatic VLDL-triglyceride production is significantly reduced in apoE-deficient mice but normalized upon human apoE3 expression, whereas the secretion rate of apoB is not affected in either of these mouse strains (35, 36). Accordingly, the average size of secreted VLDL particles produced by apoE-deficient hepatocytes is significantly reduced compared with those of wild type mice concomitant with an accumulation of small lipid droplets that colocalize with apoE within the lumen of a membrane-bound compartment. These data thus suggest that triglyceride-rich VLDL results from an apoE-dependent fusion process of triglyceride-poor VLDL with luminal lipid droplets. ApoB and apoE are considered as the major proteins mediating VLDL and LDL endocytosis by binding to the LDL receptor or the apoE receptor (34).

Lipoproteins have been shown to be of relevance for assembly and release of HCV particles (21, 37). However, the nature of the interaction between these cellular components and viral particles as well as the lipid composition and morphology of HCV remain elusive. In this study, we developed a simple and highly efficient method to produce large amounts of purified infectious HCV particles, and we performed a comprehensive analysis of infectious HCV, including the determination of its morphology and lipid composition.

EXPERIMENTAL PROCEDURES

Antibodies—A detailed list of antibodies used in this study is given in supplemental Table S1.

Cell Culture—Huh7.5 cells were used for all virus productions. Cell monolayers were grown in DMEM (Invitrogen) supplemented with 2 mM L-glutamine, nonessential amino acids, 100 units of penicillin per ml, 100 μg of streptomycin per ml, and 10% fetal calf serum (complete DMEM). Cells were routinely passaged twice a week at a split ratio of 1:7.

Plasmid Construction—Construct pFK-J6/C3 (encoding for Jc1 WT) has been described elsewhere (12, 38). To generate the Jc1 derivative encoding a FLAG-E2 fusion protein, we performed overlap PCR using two primer sets as follows: S_E1_BsiWI_J6 (5′-GGA CAT GAT GAT GAA CTG G-3′) and A_E1_FLAG (5′-CCC TTG TCA TCG TCG TCC TTG TAG TCC GCG TCC ACC CCG GCG GCC-3′); S_E1_FLAG (5′- GGA CGA CGA TGA CAA GGG ATC AGG AGC ACG CAC CCA TAC TGT TGG GGG-3′) and A_E2_XbaI (5′-CAT TGC AGC TAG CTG CGC TCG C-3′). Amplicons were combined by overlap PCR using primers S_E1_BsiWI_J6 and A_E2_XbaI, and the fragment was inserted into the Jc1 wild type construct. The resulting plasmid is designated pFK_J6/C-846/XbaI/3′-JFH1_dg_FLAG-E2 and the HCV genome transcribed therefrom is called $Jc1E2^{FLAG}$.

In Vitro Transcription and RNA Transfection—PFK-based plasmids (39) were linearized by restriction with MluI and purified using the Nucleospin Extract II kit (Macherey-Nagel, Düren, Germany). Synthesis of *in vitro* transcripts has been described in detail elsewhere (40). Concentration of purified RNA was determined by photometry, and integrity of the transcripts was verified by agarose gel electrophoresis. Transcripts were stored as 10-μg aliquots at −80 °C for further use. For RNA transfection, subconfluent Huh7.5 cell monolayers were detached from the culture dish by trypsinization, washed once with PBS, and resuspended at a concentration of 1.5×10^7 cells per ml in cytomix containing 2 mM ATP and 5 mM glutathione (41). Ten micrograms of *in vitro* transcript was mixed with 400 μl of the cell suspension and transfected by electroporation at 960 millifarads and 270 V using a Gene-Pulser system (Bio-Rad) and a cuvette with a gap width of 0.4 cm (Bio-Rad). Immediately after electroporation, cells were resuspended in complete DMEM and seeded as required.

Quantification of HCV RNA by qRT-PCR—Total RNA was extracted by using a total RNA and protein isolation kit (Macherey-Nagel) according to the manufacturer's instructions. Viral RNA was quantified by qRT-PCR using the One-step RT-PCR kit (Qiagen, Hilden, Germany). In brief, 15 μl of reaction mixture contained 0.6 μl of enzyme mixture, 1.5 mM of $MgCl_2$, 1.3 μM of each specific primer (forward primer, 5′-TCT GCG GAA CCG GTG AGT A-3′; reverse primer, 5′-

GGG CAT AGA GTG GGT TTA TCC A-3′), 0.67 mM of each dNTP, 0.27 μM of HCV-specific probe, 5 μl of template RNA and RNase-free water. To determine absolute RNA amounts, a serial dilution of an RNA standard (10^2 to 10^7 HCV RNA copies per reaction) was processed in parallel. Reactions were performed on a PRISM® 7000 sequence detection system (AB Biosystems, Darmstadt, Germany) using the following program: 50 °C for 30 min, 95 °C for 15 min and 40 cycles as follows: 94 °C for 15 s, 55 °C for 30 s, and 72 °C for 30 s.

Quantification of HCV Core Protein, ApoAI, ApoB, and ApoE by ELISA—HCV core protein was quantified using the Trak C Core ELISA kit (Wako Chemicals GmbH, Neuss, Germany) according to the instructions of the manufacturer. Culture supernatants were diluted as required prior to measurement. For quantification of apoAI, apoB, or apoE, microlon 96-well plates (Greiner Bio-One GmbH, Frickenhausen, Germany) were used in combination with an apoAI (3710-1H-6), apoB (3715-1H), or apoE (3712-1H) ELISA kit (MAbtech, Hamburg, Germany). Sample processing and measurements were carried out as recommended by the manufacturer.

Immunohistochemical Staining and Virus Titration—Virus titers were determined as described elsewhere with slight modifications (11). In brief, Huh7.5 cells were seeded into 96-well plates and fixed 3–4 days after infection. For immunohistochemistry, we used an antibody specific for the JFH1 NS3 helicase (2E3, generated in cooperation with H. Tang, Florida State University) at a dilution of 1:100. Bound antibody was detected with a peroxidase-conjugated secondary antibody specific to murine IgG (Sigma) diluted 1:200 in PBS. Virus titers (50% tissue culture infective dose per ml ($TCID_{50}$/ml)) were calculated based on the method of Spearman (42) and Kärber (43).

Virus Neutralization Assay—Cell culture supernatants of Huh7.5 cells that had been electroporated with 10 μg of *in vitro* transcripts of Jc1 or $Jc1E2^{FLAG}$ were used for infection of Huh7.5 cells at a multiplicity of infection of 1–2 $TCID_{50}$/cell for 24 h. Supernatants were collected 72 and 96 h post-infection, concentrated by PEG-8,000 precipitation, and subjected to OptiPrep density gradient ultracentrifugation as described below. One-milliliter fractions were collected from the top, and 100 μl of each fraction was used to infect 7×10^4 Huh7.5MAVS-gfpNLS cells (44) that had been seeded per well of a 24-well plate. Cells were pretreated with a 1:20 dilution of an SR-BI antibody or the corresponding isotype-matched control for 1 h at 37 °C prior to infection. Twenty four hours later, cells were fixed with 2% paraformaldehyde and analyzed by fluorescence microscopy. Alternatively, PEG-8,000 concentrated $Jc1E2^{FLAG}$ preparations or affinity-purified virus was used for neutralization experiments in a $TCID_{50}$-based readout. Antibodies specified in supplemental Table S1 were added to virus preparations and incubated for 1 h at room temperatur prior to inoculation of cells.

Virus Capture Assay—For pre-adsorption of antibodies to protein G-Sepharose beads (Sigma), 10 μl of resin were mixed with a 1:50 dilution of an antibody in a total volume of 500 μl of PBS and incubated overnight at 4 °C. The following antibodies were used: anti-E2 (J6E2, AP33 (45) and 1:7 (46)), anti-apoAI (Millipore), anti-apoB (Calbiochem and Chemicon), anti-apoCI (AbCam), anti-apoE (Millipore and Progen), and a Dengue virus (DENV) envelope glycoprotein-specific antibody (see supplemental Table S1 for detailed information). Beads were washed three times with PBS and used for virus capture assay. Samples containing equal amounts of HCV RNA copies (2×10^6) were added to the antibody-coated beads and incubated for 3 h at room temperature. Immunocomplexes were pelleted for 1 min at 700 × *g* and washed four times with 1 ml of PBS. Captured viral RNA was extracted from the immunocomplexes and quantified by qRT-PCR.

Negative Staining and Immunogold Labeling for Electron Microscopy—Virus samples were fixed with 2% paraformaldehyde (Electron Microscopy Sciences (EMS), Hatfield, PA) and in some cases additionally with 2% paraformaldehyde and 0.5% osmium tetroxide (EMS) for 30 min. Five-microliter droplets of fixed virus sample were adsorbed to glow discharged carbon- and pioloform-coated 300 mesh copper grids (Science Services GmbH, Munich, Germany) for 1 h at room temperature. Upon reduction of droplet volume by evaporation, an additional 5-μl droplet of virus preparation was added to the grid. After washing the grids once with PBS, the remaining aldehyde groups on the grids were blocked with 30 mM L-glycine for 10 min at room temperature. Prior to immunogold labeling, grids were incubated with 0.8% bovine serum albumin (Roth, Karlsruhe, Germany) and 0.1% fish skin gelatin (Sigma) in PBS, 0.01% Tween 20 (blocking reagent) for 10 min. All incubation steps were performed by floating the grids on top of the droplets. For immunolabeling, antibodies were diluted in blocking reagent and incubated by floating the grids on top of 5-μl droplets for 30 min to 1 h, depending on the antibody (rabbit polyclonal J6E2 1:10, mouse monoclonal E2-AP33 1:10, rabbit polyclonal anti-FLAG (Sigma) 1:50, and rabbit monoclonal apoE (AbCam) 1:10). After washing four times with PBS, bound rabbit antibodies were detected by floating grids on colloidal 10 or 15 nm protein A gold suspensions (Cell Microscopy Center, Utrecht, The Netherlands) diluted 1:70 with blocking reagent for 1 h. For detection of mouse antibodies, a rabbit anti-mouse bridging antibody (Dako Cytomation, Hamburg, Germany) was used. After washing four times with PBS, samples were fixed with 1% glutaraldehyde in PBS for 5 min. For double immunogold labeling, the procedure was repeated using a different combination of antibody and protein A gold. After the final glutaraldehyde fixation step, grids were washed four times in PBS, six times in water, and floated on droplets containing 3% uranyl acetate (EMS) in water, or different combinations of 3% uranyl acetate, 1% osmium tetroxide (EMS), and 1.7% methyl cellulose (EMS) for 10 min. After removal of excess negative staining solution, grids were analyzed in a Zeiss EM-10 transmission electron microscope with a built in Gatan MultiScan™ camera (Gatan GmbH, Munich, Germany). Images were analyzed with the Digital Micrograph™ software and further processed by using the Adobe Photoshop software package.

SDS-PAGE and Western Blot—Proteins were heated for 20 min at 95 °C in sample buffer (125 mM Tris/HCl, 2% (w/v) SDS, 5% (v/v) 2-mercaptoethanol, 10% (v/v) glycerol, 0.001% (w/v) bromphenol blue, pH 6.8) and separated by 12% SDS-

PAGE. Proteins were electrotransferred onto a polyvinylidene fluoride (PVDF) membrane (PerkinElmer Life Sciences) for 1 h. Membrane was blocked overnight in PBS supplemented with 0.5% Tween (PBS-T) and 5% dried milk (PBS-M) at 4 °C prior to 1 h of incubation with primary antibody diluted in PBS-M. Membrane was washed three times with PBS-T and incubated for 1 h with horseradish peroxidase-conjugated secondary antibody diluted 1:10,000 in PBS-M. Bound antibodies were detected after three times washing with the ECL Plus Western blotting detection system (GE Healthcare). Silver staining was done using a ProteoSilver™ Plus silver stain kit according to the recommendations of the manufacturer.

Lipid Analysis—Samples were extracted following the method of Bligh and Dyer (47) in the presence of internal standards (PC (di-13:0, di-14:0, di-20:0, and di-21:0), PE (di-14:1, di-20:1, and di-21:1), PI (di-16:0), PS (di-14:1, di-20:1, and di-21:1), PG (di-14:1, di-20:1, and di-21:1), SM, Cer, and HexCer (18:1;14:0, 18:1, 17:0, and 18:1, 25:0), DAG (di-17:0), (2,2,3,4,4,6-D_6)-cholesterol, and cholesteryl ester (9:0, 18:0, and 24:1). After solvent evaporation, samples were resuspended in 20 mM ammonium acetate in methanol and analyzed by mass spectrometry as described previously (48–50). Briefly, lipid quantifications were performed in positive ion mode on a triple-stage quadrupole tandem mass spectrometer (QII, Micromass) equipped with a nano-ESI source (Z spray). Argon was used as collision gas at a nominal pressure of 2.5×10^{-3} millibars. The cone voltage was set to 30 V (50 V for PC analysis). The quadrupoles Q1 and Q3 were operated at unit resolution. Detection of PC, SM, Cer, HexCer, and cholesteryl esters was achieved by precursor ion scanning for the fragment ion *m*/*z* 184 (PC and SM), *m*/*z* 264 (Cer and HexCer), or *m*/*z* 369 (cholesteryl esters). PE, PI, PS, PG, DAG, and cholesterol measurements were carried out by scanning for neutral losses of *m*/*z* 141 (PE), *m*/*z* 277 (PI), *m*/*z* 185 (PS), *m*/*z* 189 (PG), *m*/*z* 35 (DAG), and *m*/*z* 77 (cholesteryl acetate), respectively. Quantitations were performed as described previously (51), except for cholesterol and cholesteryl esters (52). Quantitative lipid data were obtained for HCV particles and for controls. Lipid amounts quantified in controls were subtracted as background from those quantified in HCV preparations. In case of phosphatidylinositol and phosphatidylserine, only the major lipid species phosphatidylinositol 38:4 and phosphatidylserine 36:1 remained after background subtraction. Unsaturated phosphoglycerolipid standards and sphingolipid standards were synthesized and purified via HPLC as described previously (50, 53). Saturated PC and PI standards were purchased from Avanti Polar Lipids (Alabaster, AL); 1,2-Diheptadecanoin standard (99% purity) was from Larodan Fine Chemicals; deuterated cholesterol standard (97–98% purity) was from Cambridge Isotope Laboratories, and cholesteryl ester standards (≥95% purity) were from Sigma.

Large Scale Production of HCV Particles by Infection—Twenty four hours prior to infection, 5×10^6 Huh7.5 cells were seeded in a 15-cm diameter culture dish. The next day, cells were infected at a multiplicity of infection of 2 $TCID_{50}$/cell for 24 h. Supernatants were collected 72 and 96 h later, pooled, and filtered through a membrane with a pore width of 0.45 μm (Millipore, Schwalbach, Germany). Filtrate was concentrated by ultrafiltration using a centrifugal filter device (Centricon Plus-70, Millipore) to reduce the volume ~50-fold. Alternatively, virus was concentrated by polyethylene glycol 8000-based precipitation as described previously (11).

Gradient Purification of HCV Particles—A maximum of 35 ml per SW28 ultracentrifuge tube (Beckmann Coulter) of concentrated culture supernatant was loaded on top of a 3-ml 80% Optiprep (Axis Shield, Oslo, Norway) cushion and centrifuged at 96,281 × *g* for 20 h at 4 °C. In the case of culture supernatants of transfected Huh7.5 cells, an additional 4 ml of a 10% Optiprep phase was layered between the 80% cushion and the concentrated supernatant. After 20 h of centrifugation, 6 ml, including the 80% cushion, were collected from the bottom of the tube and subjected to floatation gradient using a preformed Optiprep/PBS step gradient (80, 60, 20, and 0%). Samples from the first ultracentrifugation, containing ~40% Optiprep from the first ultracentrifugation step, were layered between the 60 and 20% fractions and centrifuged for 20 h at 4 °C and at 96,281 × *g*. Fractions of 2 ml were harvested from the top of the tube and used for biochemical and morphological analyses as specified in the text.

Affinity Purification by Using FLAG-specific Antibodies—Concentrated virus preparations obtained from transfected Huh7.5 cells were incubated with a 0.5-ml bed volume of a FLAG M2 affinity gel (Sigma) on a spinning wheel for 3 h at room temperature. The gel was pelleted at 250 × *g* and washed three times with PBS each using a 20-fold excess of the bed volume. Bound virus was eluted in five iterative cycles using 2 bed volumes of 100 μg/ml FLAG peptide for each cycle (Sigma). Eluates were pooled and used for further characterization.

RESULTS

Association of HCV Particles with Apolipoproteins—To elucidate the controversy as to whether HCV particles are associated with apolipoproteins, especially apoB and apoE, a concentrated Jc1 virus stock was subjected to density gradient centrifugation, and fractions were analyzed by Western blot (Fig. 1*A*). In agreement with a very recent report (55), we observed a slight shift between the peak of core protein (1.13 g/ml) and E2 protein (1.10 g/ml). ApoE was detected preferentially in fractions of higher density.

Given the interaction of apoE with NS5A (22, 23, 56) and the important role of cyclophilin A (CypA) for HCV replication and assembly (57–59) we also probed the density fractions for the presence of these two proteins. In fact, both proteins were detected in these density gradient fractions, with the NS5A peak coinciding with the E2 peak, whereas CypA amounts were highest in fractions containing the highest core protein amounts. These data suggested that NS5A and CypA are either associated with HCV particles or contaminants corresponding to viral replicase complexes released from HCV-containing cells and cosedimenting to densities that are similar to HCV particles, for example (60).

Functional analyses of gradient fractions revealed the highest infectivity titers in fractions with densities of 1.05–1.11 g/ml (Fig. 1*B*, *panel 1*) containing also the majority of total infectivity (Fig. 1*B*, *panel 3*). The density distribution of viral

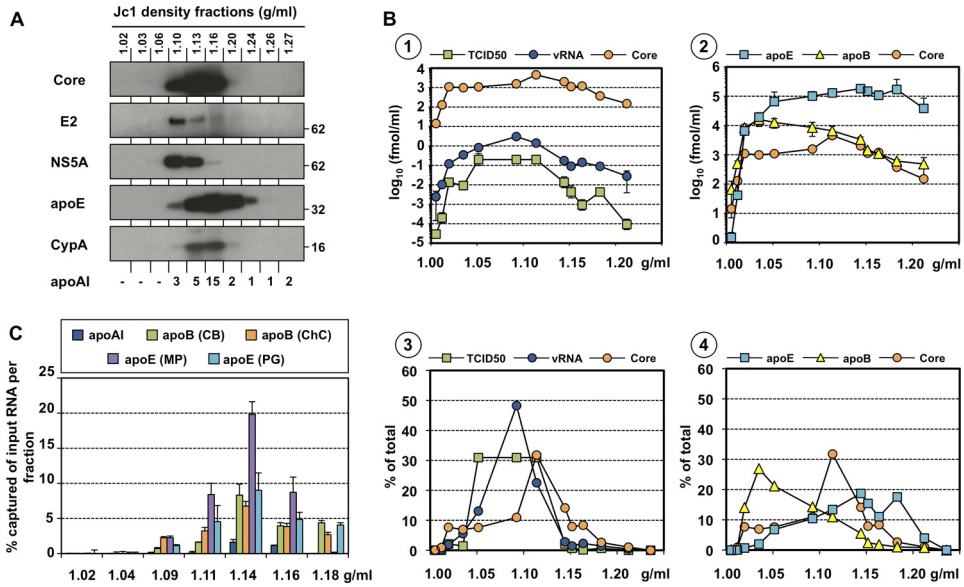

FIGURE 1. **Biochemical characterization of Jc1 particles.** Huh7.5 cells were infected with an multiplicity of infection of 2 $TCID_{50}$/cell for 24 h, and culture supernatants were collected 72 and 96 h later. Supernatants were concentrated by ultrafiltration, and concentrates were subjected to ultracentrifugation by using a 0–80% Optiprep density gradient. *A,* Western blot analysis of each density gradient fraction by using antibodies specified at the *left*. The blot is based on a preparation that was generated independently from the ones shown in *B* and *C*. As apoAI protein levels were too low for detection by Western blot, absolute amounts of apoAI as determined by ELISA are given at the *bottom* (fmol/ml). *Numbers* to the *right* refer to the apparent molecular weight of protein size marker loaded onto the same gel. *B,* for each fraction, viral RNA, infectivity titer, and amounts of core protein, apoB, and apoE were determined. Results shown in *panels 1* and *2* were obtained with the same gradient; core protein amounts are shown in both panels for ease of comparison only. Mean values and standard deviations of at least two measurements within one representative experiment are shown. Total amounts of HCV RNA, core protein, infectivity, apoB, or apoE contained in all gradient fractions shown in *panels 1* and *2* were each set to 100% to calculate the relative values that are plotted against the density of the fractions (*panels 3* and *4*). *C,* equal amounts of Jc1 particles (corresponding to 2×10^6 HCV RNA copies) contained in fractions of densities specified in the bottom were subjected to immuno-capture assay by using antibodies denoted in the legend on the *top*. In case of apoB- and apoE-specific antibodies, two different commercial sources were used, respectively (*CB,* Calbiochem; *ChC,* Chemicon; *PG,* Progen; *MP*, Millipore; for details see supplemental Table S1.). An antibody specific for the envelope protein of DENV served as a negative control and was used to determine the assay background and for normalization. HCV RNA contained in each captured sample was quantified by qRT-PCR and normalized to the capture efficiency of the negative control of the respective fraction. *Error bars* represent S.E. of duplicate measurements. A representative example of three independent experiments is shown.

RNA was overall comparable, but when normalized to the total HCV RNA contained in the virus preparation, a pronounced peak at a density of 1.10 g/ml became visible (Fig. 1*B*, *panel 3*). Of note, viral RNA amount was on average ~10-fold higher than the $TCID_{50}$ titer in a given fraction indicating an ~10-fold excess of noninfectious particles (Fig. 1*B*, *panel 1*). However, this average ratio varied along the density from as high as ~300 viral RNAs per $TCID_{50}$ in fractions where only very low infectivity could be detected (1.21 g/ml) to 4 viral RNAs per $TCID_{50}$ in fractions of high specific infectivity (1.05 g/ml). Because fractions after mere density gradient purification are likely to contain high amounts of cosedimented lipoproteins that are constitutively secreted from cells, the ratios of apoB and apoE per viral RNA or $TCID_{50}$ were extremely high (Fig. 1*B*, *panels 2* and *4*).

Having characterized these virus fractions, we next assessed the association of HCV particles contained in these fractions with apolipoproteins by using capture assays with antibodies specific for apoAI, apoB, and apoE. Of note, for each capture assay, we used the same amount of HCV RNA copies (2×10^6) allowing us to determine the relative capture efficiency and thus providing a means to assess the relative degree of association of HCV with each of these apolipoproteins. HCV RNA was efficiently captured with antibodies directed against both apoB and apoE (Fig. 1*C*). Interestingly, highest capture efficiency was obtained with an apoE-specific antibody when using the fractions with densities ranging from 1.11 to 1.16 g/ml. ApoB-specific capture was less efficient, arguing that HCV particles of the respective density contain lower amounts of this protein. The apoAI-specific antibody recovered only ~2% of the input RNA in any fraction. Capture efficiency with any of the three different HCV E2-specific antibodies was at background level (data not shown). In summary, these data suggest a strong association of HCV particles with apoE and to some extent with apoB and that these apolipoproteins play an important role for HCV infectivity.

Production of HCV Particles by Using a Jc1E2^{FLAG}-tagged Genome—Membranous HCV replication complexes (60) and lipoproteins secreted from cells are difficult to separate from HCV particles by ultracentrifugation and gel filtration because of their similar biophysical properties. Therefore, we performed affinity purification, initially by using antibodies specific for the E2 protein. However, capture efficiencies were too low and virus amounts were not sufficient for biochemical assays (data not shown). For this reason, we fused a FLAG tag to the N terminus of the E2 protein in the context of our Jc1 chimera (Fig. 2*A*) to allow immuno-capture with a high avidity FLAG antibody system. As shown in Fig. 2*B*, addition of this tag neither affected the kinetics nor the absolute amounts of infectious virus production as compared with wild type Jc1. Likewise, the density distribution of infectivity obtained with these two genomes was comparable with the exception that

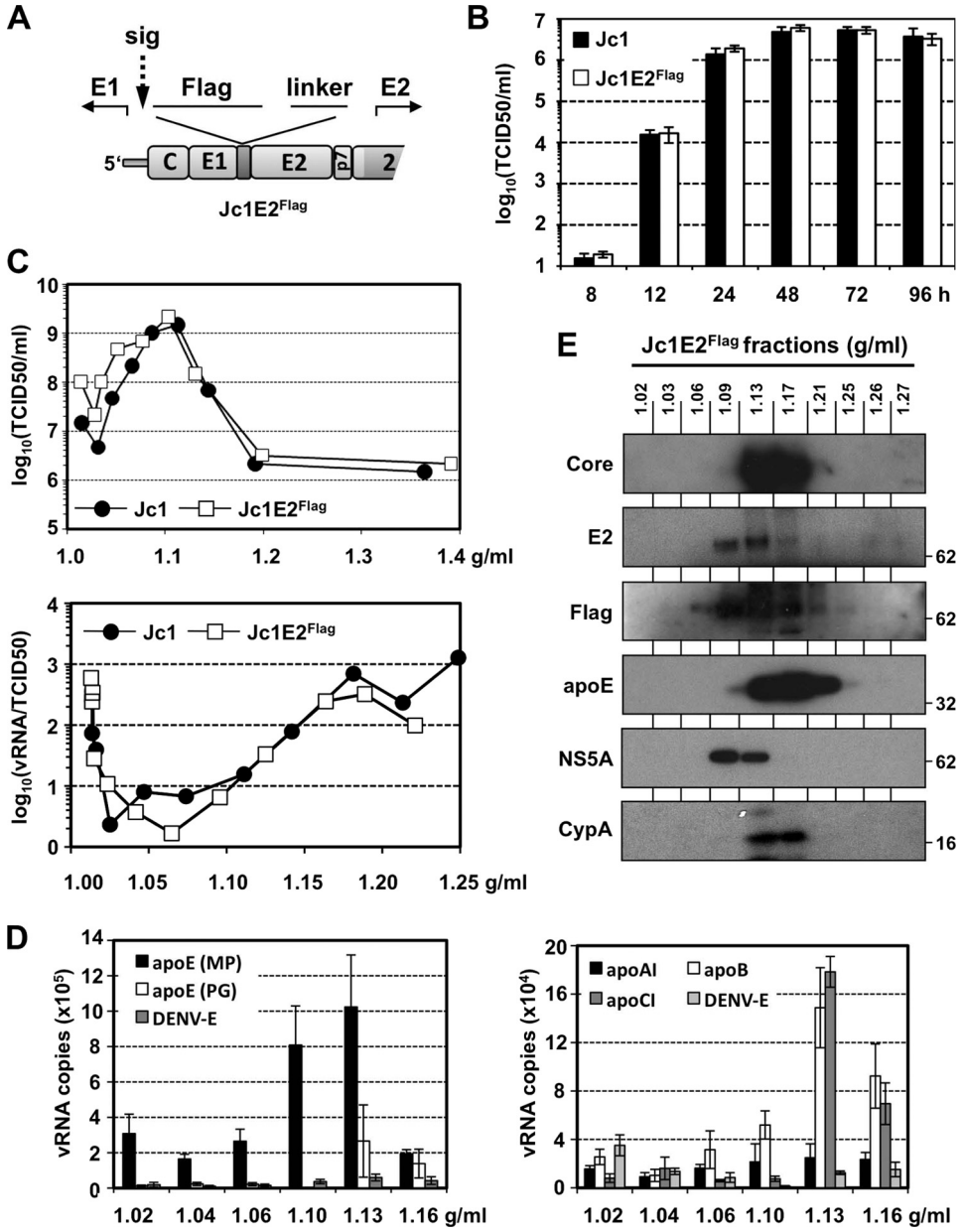

FIGURE 2. **Comparison of Jc1 and Jc1E2^{FLAG} particle production and analysis of density profiles.** *A,* schematic representation of the Jc1E2^{FLAG} virus genome and amino acid sequence of the fusion site. The putative signalase cleavage site (*sig*) is indicated with a *dotted arrow*. *B,* comparative analysis of the kinetics of infectivity release from Huh7.5 cells after transfection with Jc1 or Jc1E2^{FLAG}. Virus titers were determined by $TCID_{50}$ assay. Note the indistinguishable production kinetics and amounts of infectious virus achieved with the two HCV genomes. *Error bars* represent standard deviations of two measurements. *C, upper panel,* density distribution of infectious Jc1 and Jc1E2^{FLAG} particles. A representative example of two independent experiments is shown. *Lower panel,* vRNA and infectivity of Jc1 and Jc1E2^{FLAG} contained in density fractions were determined by qRT-PCR or $TCID_{50}$ assay, respectively. The ratios of vRNA and $TCID_{50}$ indicating specific infectivity were calculated. *D,* lipoprotein association of Jc1E2^{FLAG} as determined by immuno-capture. In brief, 1×10^7 (*left*) or 2×10^6 vRNA (*right*) per fraction were used for immuno-capture with antibody-coated protein G-Sepharose beads for 4 h at 4 °C, and capture efficiency was assessed by qRT-PCR. Antibodies are specified at the *top* and densities of gradient fractions at the *bottom*, respectively. The DENV-E antibody served as a negative control. *Error bars* indicate standard deviations of triplicate measurements. Two different apoE-specific antibodies that are described in supplemental Table 1 were used. *E,* Jc1E2^{FLAG} released from Huh7.5-transfected cells was concentrated by ultracentrifugation and used for density gradient centrifugation. Fractions with densities given at the *top* were analyzed by Western blot using antibodies specified on the *left*. *Numbers* to the *right* refer to the apparent molecular weight of protein size marker loaded onto the same gel.

the tagged virus produced slightly higher infectivity in lower density fractions (Fig. 2*C*, *upper panel*) arguing for an altered propensity of the tagged E2 to interact with lipids or to utilize SR-BI. In fact, by using neutralization studies, we found that Jc1E2^{FLAG} is less susceptible to SR-BI neutralization as compared with Jc1 (supplemental Fig. S1). This result indicated altered binding of the tagged E2 to SR-BI and presumably enhanced entry into Huh7.5 cells that were used for $TCID_{50}$ assay. Specific infectivity proved to be slightly different between Jc1 and Jc1E2^{FLAG} at low buoyant density (Fig. 2*C*, *lower panel*), but infectivity was enriched in both cases in the 1.1 g/ml density fraction. Finally, association of Jc1E2^{FLAG} with lipoproteins as determined by immuno-capture was comparable with the one of Jc1 (compare Fig. 2*D* with 1*C*).

To determine the density distribution of viral and cellular proteins, we subjected a concentrated Jc1E2^{FLAG} virus stock to ultracentrifugation using an Optiprep density step gradient in the exact same way as applied for Jc1 wild type (Fig. 1*A*). We found that also in case of the tagged virus, CypA and NS5A cosedimented with virus particles, and the density profiles of structural proteins as well as of apoE, NS5A, and CypA were virtually identical to those obtained with Jc1 wild type samples (compare Fig. 1*A* with 2*E*). Again, we observed a slight density shift between the peaks of the core protein and E2, which was confirmed by a FLAG-specific antibody, and cosedimentation of NS5A and E2 as well as CypA and core, respectively (Fig. 2*E*). In summary, these data show that particles produced with the Jc1E2^{FLAG} genome are comparable with those generated with Jc1 wild type and can be efficiently enriched by immuno-capture.

Characterization of Affinity-purified HCV Particles—Taking advantage of the Jc1E2^{FLAG} genome, we generated large amounts of HCV particles by electroporation of Huh7.5 cells and subsequently concentrated virus in culture supernatants by ultrafiltration or polyethylene glycol-based precipitation (Fig. 3*A*). Virus in concentrates was purified by sedimentation onto an Optiprep cushion. In the initial set of experiments, samples from the top of the cushion were subjected to density gradient centrifugation as described in Fig. 1 prior to affinity purification, but virus yields were too low to allow for biochemical analyses of HCV particles (data not shown). Therefore, samples from the first ultracentrifugation were directly subjected to affinity purification using commercially available FLAG-M2 beads, and captured virus was eluted by using a FLAG peptide (for details see under "Experimental Procedures"). Jc1 wild type was processed in parallel and used as a specificity control. As summarized in Fig. 3*B*, we could recover ~50% of the Jc1E2^{FLAG} input infectivity in the eluate, whereas infectivity titers in the Jc1 affinity preparation were more than 10^5-fold reduced as compared with the input demonstrating high specificity of the affinity purification procedure.

When affinity-purified preparations were analyzed on a silver-stained protein gel, the degree of purification became immediately evident (Fig. 3*C*). The majority of proteins present in the input used for affinity purification was absent in the eluate (Fig. 3*C*). Only a few bands were detectable in the eluate, but no difference was observed between Jc1 and Jc1E2^{FLAG} arguing that amounts of viral proteins were still too low for detection with this method. However, ~50% of total infectivity was still retained in the Jc1E2^{FLAG} eluate (Fig. 3*B*), demonstrating strong enrichment of the virus.

In affinity-purified Jc1E2^{FLAG} preparations, core proteins E2 and apoE were readily detected by Western blot (Fig. 3*D*). Moreover, E2 protein was also detected with the FLAG-specific antibody. Most notably, both NS5A and CypA were no longer detected in this virus preparation, although both proteins were readily detected in Huh7.5 cells in which the two virus preparations had been produced (Fig. 3*D*). Therefore, we conclude that neither NS5A nor CypA are major constituents of HCV particles. Because of its large size (512 kDa), we used an ELISA instead of SDS-PAGE to quantify apoB, but

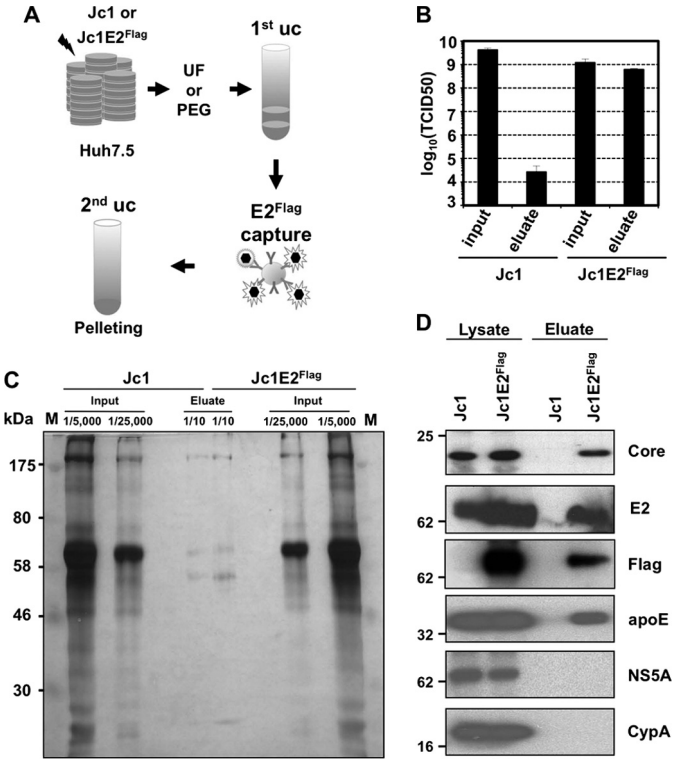

FIGURE 3. **Biochemical characterization of affinity-purified Jc1E2^{FLAG} particles.** *A,* schematic representation of Jc1E2^{FLAG} virus production and purification. Culture supernatants of transfected cells were concentrated by ultrafiltration (*UF*) or PEG precipitation (*PEG*) and purified by sedimentation onto an 80% Optiprep cushion. Samples collected from the *top* of the cushion were used for FLAG-affinity purification, and eluted particles were subjected to a final concentration by ultracentrifugation. *B,* infectivity in fractions specified at the *bottom* was determined by $TCID_{50}$ assay. Note the ~10^5-fold loss of infectivity after affinity capture in case of Jc1 and the high recovery in the case of Jc1E2^{FLAG} particles. *C,* silver gel analysis of Jc1 and Jc1E2^{FLAG} preparations before (*Input*) and after affinity purification (*Eluate*). Ratios given at the *top* of the panel refer to fractions of each sample loaded onto the gel. Note the massive reduction of total protein in the eluate. *Numbers* at the *left* refer to the apparent molecular weight of protein size marker (*M*) loaded onto the same gel. *D,* Western blot analysis of Jc1 and Jc1E2^{FLAG} after FLAG-affinity purification. Supernatants of transfected Huh7.5 cells were processed as described in *A,* and eluates were subjected to Western blot with antibodies specified on the *right.* Lysates of transfected cells were loaded in parallel for comparison. Note the absence of NS5A and CypA in affinity-purified samples. Because of very low binding to the FLAG-affinity beads, no viral proteins are detectable in case of the Jc1 sample.

after affinity purification, this protein was below the detection limit of the assay (~40 fmol/ml).

When calculating the ratio of viral RNA to infectivity as determined by the $TCID_{50}$ assay, we found a remarkable shift. Whereas in unpurified preparation or fractions concentrated by ultracentrifugation, the ratio of RNA to infectious particles was ~10:1, this ratio shifted to ~2:1 after affinity purification. This shift likely reflects the removal of noninfectious RNA-containing particles, which might be caused by a selective enrichment of particles with a high abundance of FLAG-tagged yet fully functional E2 protein (see "Discussion").

Role of Apolipoprotein E for Infectivity of HCV Particles—The availability of purified infectious HCV particles allowed for the analysis of the role of apolipoproteins for infectivity. To this end, we performed comparative neutralization experiments of Jc1E2^{FLAG} particles before and after affinity purification. Control antibodies specific for E2 or the FLAG tag po-

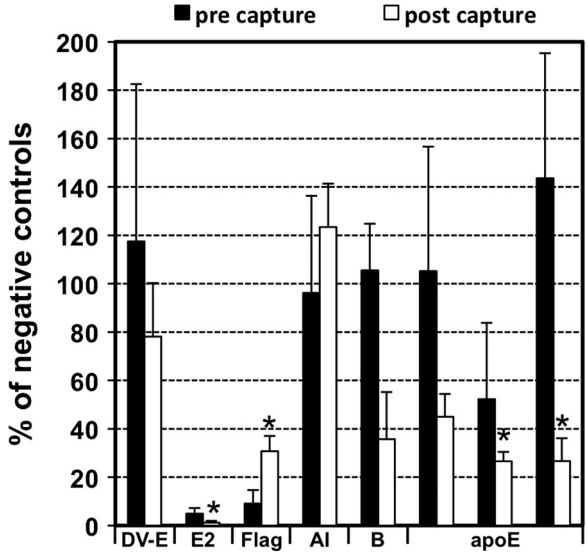

FIGURE 4. **Comparative analysis of neutralization of Jc1E2^{FLAG} before and after affinity purification.** Concentrated (pre-capture) or affinity-purified (post-capture) Jc1E2^{FLAG} samples were incubated with antibodies specified at the *bottom* for 1 h at room temperature and added to Huh7.5 cells. Infection of cells was determined 72 h after inoculation by using $TCID_{50}$ measurement. The means of three independent experiments are shown. Data were normalized to the mean values of three negative controls (untreated, antibodies specific for DV-E protein, and for calreticulin). Only *DV-E* is shown as a representative negative control. *Error bars* indicate S.E. ($n = 3$). Note that statistically significant neutralization (labeled with *) could only be achieved after affinity purification. Also note that the reduced neutralization of affinity-purified virus with the FLAG-specific antibody as compared with unpurified samples is within the variability range. Antibodies of the following specificity were used: *DV-E*, DENV-E protein; *AI*, apolipoprotein AI; *B*, apolipoprotein B; *E*, apolipoprotein E (apoE; three different antibodies).

tently neutralized infectivity, whereas the antibody against the E-protein of DENV had no effect (Fig. 4). In agreement with previous results, we found that antibodies targeting apoE and apoB, but not apoAI, neutralized infectivity, albeit to various extents. Most notable was the augmented neutralization of affinity-purified HCV by the apoE-specific antibodies ($p = 0.04$ for the CB antibody and $p = 0.05$ for the Progen antibody; $n = 3$; specification of the antibodies is given in supplemental Table S1). A moderate neutralization with the apoB-specific antibody was also detectable, but it was not statistically significant when compared with the DENV negative control. Together with the finding that HCV RNA-containing particles can be captured with apoB-specific antibodies, our data suggest that apoB is also associated with virus particles but may play a minor role during entry. Moreover, the impact of apolipoproteins on HCV infectivity is best detected after removing contaminating lipoproteins by affinity purification.

Determination of the Lipid Composition of Jc1E2^{FLAG} Particles by Using Mass Spectrometry—To determine the lipid composition of HCV, affinity-purified Jc1E2^{FLAG} particles were subjected to quantitative lipid analysis employing nano-electrospray ionization tandem mass spectrometry (Fig. 5). Jc1 wild type preparations were analyzed in parallel to control for host cell-derived background. Quantitative lipid analysis was achieved by the addition of internal lipid standards for each lipid class. Lipids detected in preparations of Jc1 were subtracted from lipids detected in Jc1E2^{FLAG} preparations to account for host cell background. As shown for the major lipids phosphatidylcholine, sphingomyelin (Fig. 5*A*), and cholesteryl ester (Fig. 5*B*), amounts of most viral lipids were significantly above background. In this way, we were able to define phosphatidylcholine, sphingomyelin, as well as cholesteryl esters and cholesterol as major lipids of HCV particles (see also supplemental Table 2). Phosphatidylethanolamine, phosphatidylserine, phosphatidylinositol, and phosphatidylglycerol were detected as minor lipids, whereas diacylglycerol, ceramide, and hexosylceramide were not detected above background. In total, 9 lipid classes (Fig. 5*C*, *left panel*, and Table 1) and 77 lipid species (supplemental Fig. S2 for lipid species distributions) were found. In comparison with other viral particles (such as HIV-1 (51), vesicular stomatitis virus, and Semliki Forest virus (61)), a striking enrichment of cholesteryl esters as nonbilayer lipids and relatively low amounts of most phospholipids were observed (Fig. 5, *C* and *D*). Although our analysis did not cover all possible lipids, most notably triacylglycerol that could not be quantified for technical reasons, the results suggest that the lipid composition of infectious HCV particles generated in Huh7.5 cells is similar to the one of LDL and VLDL (51, 61, 62).

To analyze whether the lipid composition of HCV particles reflects an unusual lipid composition of host cell membranes, we subjected Huh7.5 cells to quantitative lipid analysis and analyzed them by mass spectrometry as described above (supplemental Fig. S3). We found that the lipidome of HCV particles is strikingly different from cell membranes with the latter exhibiting much higher relative amounts of phospholipids and much lower levels of cholesteryl esters (Fig. 5*C*, *right panel,* and Table 1). In summary, these data suggest that HCV has a unique lipid composition that differs from all other viruses analyzed thus far. This lipid composition resembling VLDL/LDL particles is in full support of the tight association of HCV particles with lipoproteins, most notably apoE.

Morphological Analysis of Affinity-purified Jc1E2^{FLAG} Particles by Electron Microscopy—In our initial experiments, we studied the morphology of Jc1 wild type virus after purification by ultracentrifugation by using negative staining and transmission electron microscopy (supplemental Fig. S4). In fractions containing the highest infectivity titer (~1.1 g/ml, we detected heterogeneous structures that were most often spherical but occasionally amorphous. The sizes of these structures were variable and ranged between 31 and 125 nm (supplemental Fig. S4*D*). A fraction of these particles could be immunolabeled with E2- or apoE-specific antibodies or both (supplemental Fig. S4*B*). The average diameter of labeled structures that most likely represent HCV particles was 73 nm.

Because these density gradient fractions still contained impurities (Fig. 1), detailed and reliable analyses were difficult. We therefore generated affinity-purified Jc1E2^{FLAG} particles and re-analyzed HCV particle morphology. Examination of the samples before and after affinity purification revealed a massive reduction in the overall abundance of small spherical structures (data not shown). Moreover, the total number of structures in Jc1E2^{FLAG} samples was high, whereas almost no structures were detectable in the Jc1 control preparations (data not shown).

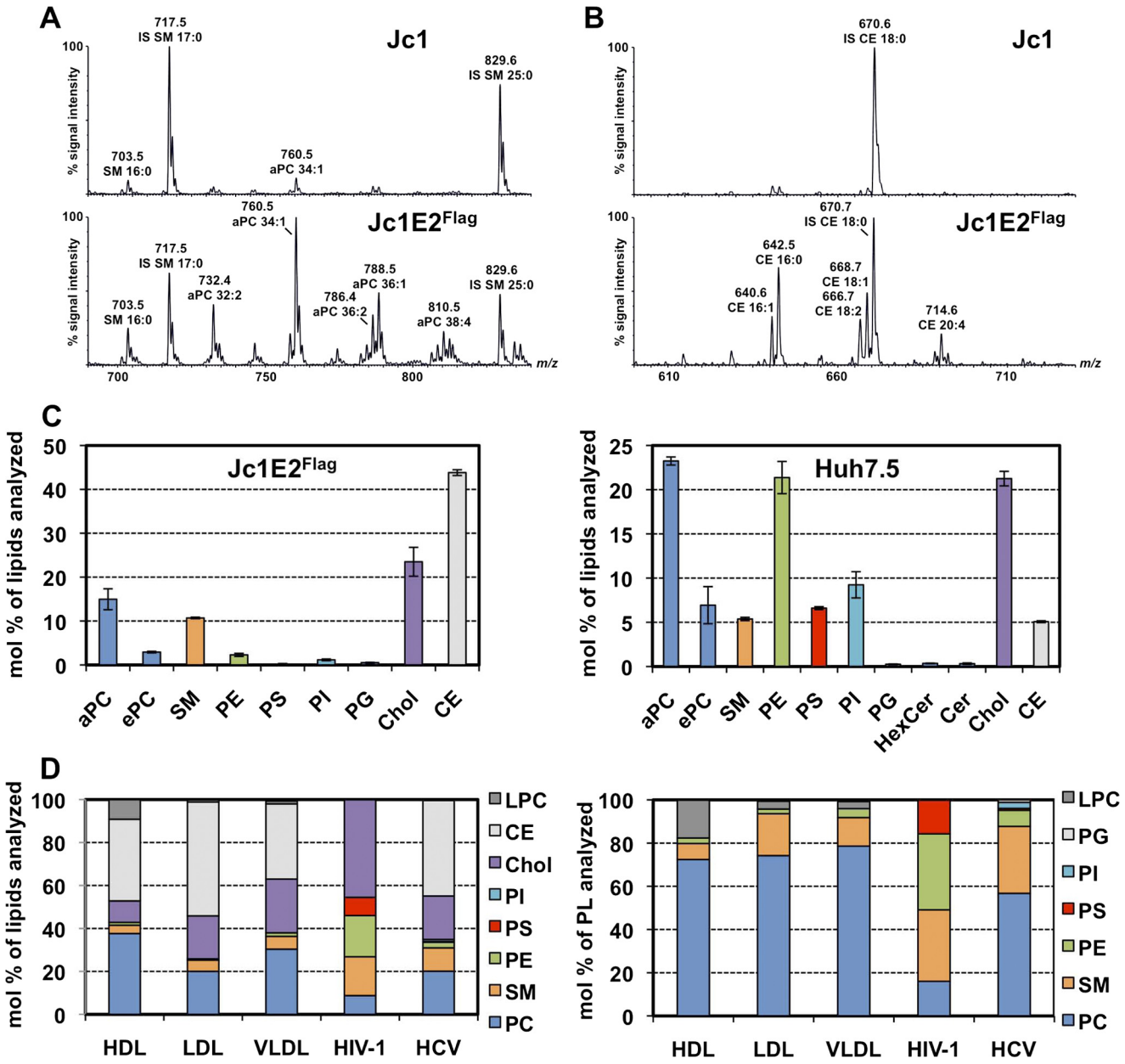

FIGURE 5. **Lipid composition of affinity-purified Jc1E2^{FLAG} particles produced in Huh7.5 cells.** Total lipids contained in affinity-purified Jc1E2^{FLAG} particles and in lysates of Huh7.5 cells transfected with the HCV genome (control) were extracted and subjected to quantitative lipid analysis by nano-ESI-MS/MS. *A,* detection of phosphatidylcholine and sphingomyelin species in the Jc1 control eluate (*upper panel*) and Jc1E2^{FLAG} viral particles (*lower panel*) (precursor ion scans of *m/z* 184). *B,* detection of cholesteryl ester species in the Jc1 control (*upper panel*) and Jc1E2^{FLAG} viral particles (*lower panel*) (precursor ion scans of *m/z* 369). Major lipid species are annotated giving number of carbon atoms/number of double bonds in fatty acids. *IS,* internal standard. *C,* lipid composition of HCV particles (*left panel*, $n = 2$) or of Huh7.5 cells (*right panel*, $n = 3$). HexCer and Cer were only detectable in Huh7.5 cells, but not in Jc1E2^{FLAG} (see Table 1). *D,* phospholipid (*right panel*) or total lipid profiles (*left panel*) of lipoprotein particles (HDL, LDL, and VLDL were taken from Ref. 62), HIV-1 (taken from Ref. 51), and HCV (from this study). *aPC,* acyl-linked phosphatidylcholine; *ePC,* ether-linked phosphatidylcholine; *SM,* sphingomyelin; *PE,* phosphatidylethanolamine; *PS,* phosphatidylserine; *PI,* phosphatidylinositol; *PG,* phosphatidylglycerol; *Chol,* cholesterol; *CE,* cholesteryl ester, *HexCer,* hexosylceramide; *Cer,* ceramide; *LPC,* lysophosphatidylcholine; *PL,* phospholipids. Triacylglycerol (*TAG*) concentrations were not determined due to technical difficulties.

Detailed morphological analyses revealed also for affinity-purified Jc1E2^{FLAG} particles a high heterogeneity (Fig. 6). The diameter of particles ranged from 28 to 152 nm ($n = 209$). Several of the observed structures displayed a positive rather than a negative staining pattern, indicating damage of the particles (Fig. 6*A*, *panels b* and *e*). Whether this is due to the preparation procedure or to the used fixation methods is unknown.

Immunolabeling Identifies ApoE as an Integral Component of HCV Particles—To identify the best conditions for structure preservation of Jc1E2^{FLAG} particles, we tested a variety of fixatives and negative staining methods, including ammonium molybdate with or without trehalose, uranyl formiate, uranyl acetate, or phosphotungstic acid (data not shown). Furthermore, we compared preservation, antigen accessibility, and contrast of different combinations of methyl cellulose, uranyl

TABLE 1

Lipid composition of Huh7.5 cells and affinity-purified Jc1E2^{FLAG} particles

Lipids were extracted and analyzed for containing lipid species as described under "Experimental Procedures." Values are expressed as mole percentage of a given lipid to total lipids quantified. aPC, acyl-linked phosphatidylcholine; ePC, ether-linked phosphatidylcholine. Mean values indicating mean ± S.E. are given.

	Huh7.5 cells ($n = 3$)	Jc1E2^{FLAG} ($n = 2$)
	mol % ± S.E.	*mol % ± S.E.*
aPC	23.24 ± 0.46	17.33 ± 2.38
ePC	6.93 ± 2.1	2.75 ± 0.17
SM	5.37 ± 0.19	10.88 ± 0.18
PE	21.37 ± 1.82	2.64 ± 0.35
PS	6.6 ± 0.17	0.32 ± 0.17
PI	9.24 ± 1.49	0.97 ± 0.19
PG	0.25 ± 0.04	0.4 ± 0.1
HexCer	0.36 ± 0.03	Below detection limit
Cer	0.32 ± 0.08	Below detection limit
Chol	21.25 ± 0.82	20.21 ± 3.29
CE	5.07 ± 0.1	44.47 ± 0.65
TAG	Not determined	Not determined

acetate, and osmium tetroxide (supplemental Fig. S5). Whereas uranyl acetate alone gave the best result for immunolabeling, the addition of osmium tetroxide preserved the structures best. However, these conditions reduced labeling efficiency probably due to antigen masking or alteration. Methyl cellulose also increased structure preservation but reduced the overall contrast (supplemental Fig. S5). Thus, uranyl acetate was the best compromise for structure preservation, contrast, and antigen accessibility, and this method was therefore used for all subsequent experiments.

By using these conditions, ~21% of all structures contained in affinity-purified samples could be labeled with a rabbit polyclonal antibody (J6E2); labeling efficiency with the mouse monoclonal antibody AP33 was much lower and therefore not quantified. Moreover, tagged virus particles also reacted with a FLAG-specific antibody (Fig. 6*A*, *panel h*). However, because of high amounts of FLAG peptide, which was used for elution of Jc1E2^{FLAG} from the M2-affinity gel, the background obtained with the FLAG-specific antibody precluded quantitative analyses of EM micrographs.

The average diameter of E2-labeled structures was 73 nm (Fig. 6, *A*, *C*, and *D*). However, in all cases labeling density was low, arguing for low amounts of E2 protein on the surface of HCV particles or for poor antigen accessibility or integrity. In contrast, a high percentage of all structures (more than 56%) could be labeled with an apoE-specific antibody (Fig. 6*D*). This result is in keeping with the notion of a high number (~300 as determined by ELISA) of apoE molecules per viral RNA copy, which may be even higher than the number of E2 molecules per particle. ApoE labeling was confined to the viral envelope confirming specificity of the antibody. Moreover, labeling background on the grids was lower than 2 gold particles per μm^2 for the J6E2 antibody and slightly above 1 gold particle per μm^2 for the apoE-specific antibody corroborating that our labeling was specific (Fig. 6*E*).

Overall, affinity-purified HCV particles did not display an ordered inner structure. Some of the E2-stained particles displayed an inner structure that was separated from the envelope by an electron translucent ring (Fig. 6*A*, *panel e*). However, attempts to characterize these particles further by using various pretreatments (*e.g.* with mild detergents or lipoprotein lipase) and antibodies detecting core or other viral or cellular proteins, including apoB, were not successful (data not shown).

By using double immunogold labeling, we were able to detect HCV-E2 and apoE on the same virus particles. In fact, ~66% of all E2-bearing particles could also be labeled for apoE (Fig. 6*D*). Importantly, the majority of E2-positive structures were singular, and only occasionally E2-positive particles were associated with particles that were not labeled (Fig. 6*F*). In summary, these data confirm the heterogeneity of HCV particle morphology, and they demonstrate that apoE is an integral component of infectious hepatitis C virions.

DISCUSSION

Affinity Purification of HCV Particles—A major obstacle for biochemical and ultrastructural analyses of infectious HCV particles is their high heterogeneity and their similarity to host cell lipoproteins. For these reasons, mere ultracentrifugation and gel filtration methods are hardly sufficient to separate the cellular and viral particle species resulting in high background of host cell lipids and proteins (14, 17, 63). In this study, we describe a simple and highly efficient method that circumvents these problems. By using a FLAG-tagged HCV that produces infectivity titers to wild type levels, in combination with affinity capture, large amounts of pure HCV particles can be generated. The power of this method is illustrated by NS5A and CypA. These two proteins are involved in HCV assembly (57, 58); they cosediment with virions in density gradients (Figs. 1*A* and 2*E*), but they are not detectable in virus fractions after affinity purification (Fig. 3*D*). We described earlier that HCV-containing cells release membranous and presumably vesicular very low density structures containing viral RNA and proteins (60). These structures, but also host cell lipoproteins constitutively secreted from cells, contaminate virus preparations and thus make specific detection of viral lipids as well as low abundance proteins in virus particles very difficult. Moreover, when Jc1E2^{FLAG} particles were used for neutralization experiments, infectivity could be efficiently neutralized with apolipoprotein-specific antibodies only after affinity purification, suggesting that the majority of free lipoprotein particles was removed by this method.

We found that the ratio of viral RNA to infectious particles was reduced from ~10:1 before affinity purification to ~2:1 thereafter, arguing that our method may select for virus particles enriched for (FLAG-tagged) E2 protein. Moreover, this shift indicates high amounts of RNA-containing noninfectious particles. The nature of these particles present in almost 10-fold excess over infectious particles in noncaptured samples is not known. They may correspond to RNA-containing nonenveloped capsids (64) to exosomes, *i.e.* membranous vesicles containing viral RNA, core, and envelope glycoproteins (65), or to replication complexes (60). Whatever the nature of these structures is, they are efficiently removed by our affinity purification. Moreover, we note that a similar approach using a 3× FLAG-tagged E2 in the context of a chimeric HCV genome has been described very recently (66). However, in this virus, part of the N-terminal HVR1 in E2 was replaced, whereas we did not delete viral sequences but rather directly

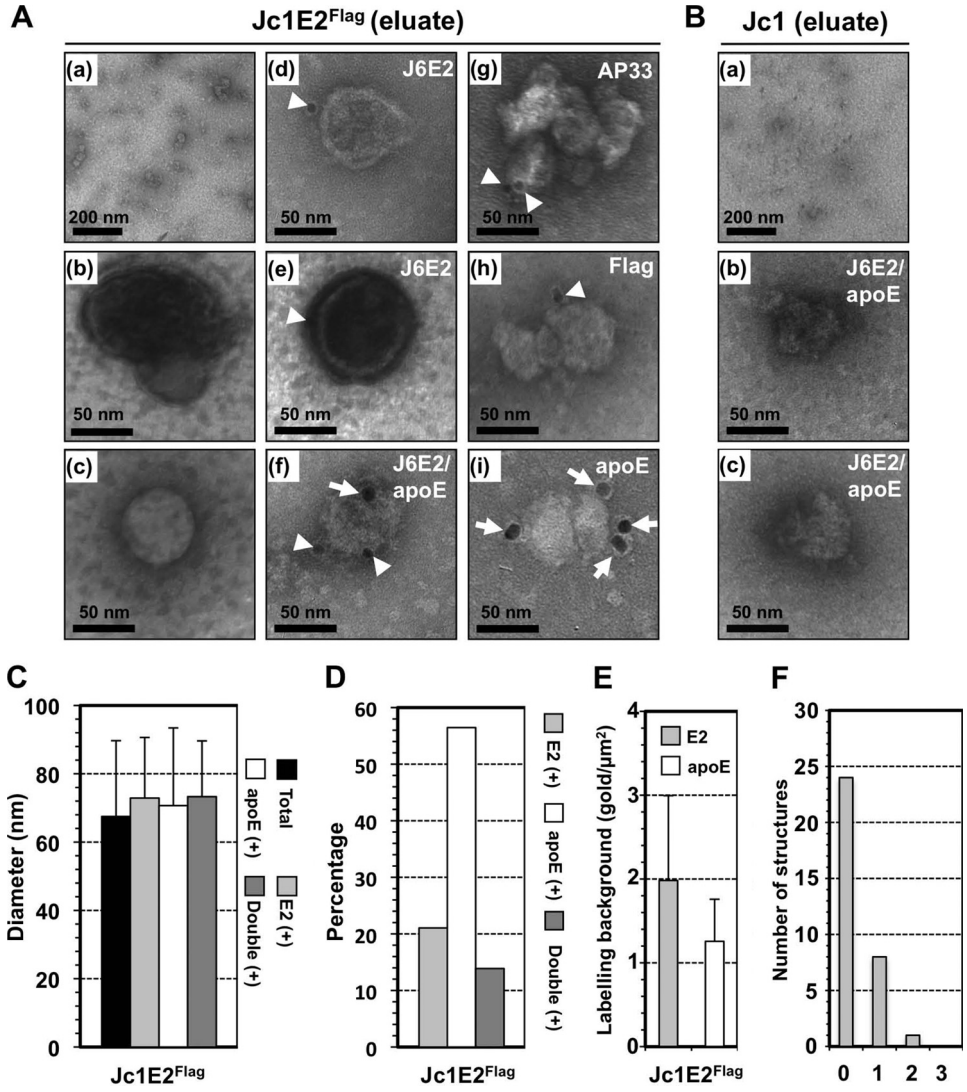

FIGURE 6. **Morphology of affinity-purified Jc1E2^{FLAG} particles as visualized by negative staining and transmission electron microscopy.** Virus contained in supernatants of transfected Huh7.5 cells was purified as described in Fig. 3*A* and under "Experimental Procedures." *A,* affinity-purified Jc1E2^{FLAG} particles were either unlabeled (*panels a–c*) or immunolabeled for the E2 envelope glycoprotein (*arrowheads*) as specified in the *upper right* of each panel, and bound antibodies were detected with 10 nm colloidal gold (*panels d–h*). ApoE was detected with a rabbit monoclonal antibody and 15 nm gold particles (*arrows* in *panels f* and *i*). *Panel f* depicts the result of double immunolabeling. *B,* culture supernatant containing high titers of Jc1 was subjected to affinity purification and used as control sample to determine specificity of immunolabeling. Although this sample also contained spherical particles, their abundance was much lower (*panel a*), and these particles did not react with the J6E2- or ApoE-specific antibodies (*panels b* and *c*). *C–F,* statistics were performed by counting structures and immunogold particles bound to each structure on at least two different EM grids of at least two preparations each. *C,* mean diameters of all counted structures (*Total*) as well as of structures that labeled with one antibody only or with both (*Double* (+)). *D,* relative proportion of structures that were labeled with either one or two antibodies. *E,* labeling background of the J6E2- or apoE-specific antibody expressed as number of gold particles per μm^2. *F,* absolute number of J6E2-labeled particles that were either singular (*0*), or associated with 1 or 2 nonlabeled particles. *Error bars* in *C–E* represent the standard deviation ($n = 209$).

fused the FLAG tag to the E2 N terminus. The construct design used in the other study may explain why the 3× FLAG-tagged virus genome is severely impaired in assembly competence and requires an adaptive mutation in E2 to compensate for this defect. Furthermore, Takahashi *et al.* (66) described HCV particles with an average diameter of 40–60 nm, whereas our own data suggest an average diameter of ~70 nm. The reason for this discrepancy is not known, but it might be due to different fixation methods, the use of different HCV recombinants, or different host cell lines utilized for virion production. In fact, lipid composition of HCV, and thus its size and density, very much depends on the host cell in which the virus is produced. For instance, HCV from primary human hepatocytes or patient sera has a much lower density and association with apoB as compared with HCV produced in Huh7 cells (16, 67–69). This "lipid imprinting" of HCV particles and its dependence on the particular host cell may explain some of the discrepant observations reported in various studies.

One disadvantage of the affinity purification is the reduced stability of infectivity after capture. Whereas HCV contained in culture supernatant retains full infectivity when stored for 1 week at 4 °C, for example (70), infectivity of captured virus samples is reduced by up to 100-fold within 16 h at 4 °C. Therefore, analyses of infectious virions after capture by using density gradient centrifugation were difficult as infectivity was

rapidly lost. Nevertheless, the density profile of infectious HCV particles was very similar before and after affinity purification arguing that infectivity, but not overall structural integrity, was affected .[7] The reason for the reduced stability is not known but could be due to rapid degradation because of the lack of excess carrier protein/lipid in the sample or to a "preactivation" of virions upon binding and removal of the FLAG-specific antibody. In this respect, the antibody may mimic an interaction with CD81, which might trigger a conformational change leading to reduced infectivity.

Infectivity distribution of Jc1E2^{FLAG} virions was slightly shifted toward lower density in comparison with Jc1. Although this observation implies that infectivity of Jc1E2^{FLAG} accumulates in fractions of 1.01–1.05 g/ml to a higher extent than with wild type, more than 85% of total infectivity for both Jc1 and Jc1E2^{FLAG} was detected in peak fractions with densities of ~1.1 g/ml. Thus, a possible difference in lipid composition of the tagged particles can only contribute to a very minor degree. Apart from that, fusion of the FLAG tag to the N terminus of HVR1 seems to have altered the propensity of E2 to interact with an SR-BI as neutralization efficiency with an SR-BI-specific antibody was reduced by 2–3-fold with Jc1E2^{FLAG} as compared with Jc1. We therefore assume that the apparent density shift of Jc1E2^{FLAG} particles is not due to particle composition, but rather might be due to altered binding of E2 to SR-BI and thus enhanced HCV entry into Huh7.5 cells that were used to measure infectivity.

Lipid Composition of Affinity-purified HCV Particles—Affinity-purified HCV particles also allowed quantification of apoE amounts. By using ELISA, we determined 290 ± 41 apoE molecules per viral RNA. Values were very reproducible, and amounts were consistently well above the detection limit of the assay. This calculation assumes that apoE is only associated with infectious HCV particles. It is possible, however, that cells secrete in addition certain amounts of subviral particles devoid of viral RNA and core but containing envelope glycoproteins, apoE, and possibly apoB. Nevertheless, it has been shown that the glycoproteins E1 and E2 do not associate with apoB when overexpressed in Huh7.5 cells (25). Therefore, it is unlikely that large amounts of E1/E2-containing particles associated with lipoproteins are present in our affinity-purified virus samples.

A key element of our study is the determination of the lipidome of HCV particles. An earlier report by Aizaki *et al.* (71) described a quantification of cholesterol and phospholipids contained in a partially purified preparation of HCV particles produced in Huh7 cells. The authors determined cholesterol to total phospholipid ratio of ~1.26 but did not monitor cholesteryl esters or discriminate between individual phospholipid species. In contrast, by using affinity-purified HCV particles, we found that phospholipids are much more abundant than cholesterol (cholesterol/phospholipids ratio ~0.59). Most importantly, the predominant lipid species of HCV particles determined in our study are cholesteryl esters, accounting for ~44% of total viral lipids. Thus, HCV appears to have a unique lipid composition that is distinct from all other viruses studied so far. Because of the specificity of our affinity purification, major lipids could be determined with high accuracy as exemplified by the mass spectra shown in Fig. 5 and supplemental Fig. S3. Overall, polar membrane lipids such as phosphatidylserine and phosphatidylethanolamine that are enriched in HIV-1 (51), vesicular stomatitis virus, or Semliki Forest virus (61) are only minor lipids in hepatitis C virions. Along these lines, cholesterol, which is thought to be important especially for viruses that acquire their envelope from the plasma membrane, where cholesterol is most abundant, was well detectable in HCV particles but to lower concentrations than in other viruses (61). Likewise, sphingomyelin is enriched in HCV particles but again to a lower extent than reported for other viruses. Likewise, the membrane of the hepatitis B virus, a virus that, similar to what has been proposed for HCV, acquires its membrane from pre-Golgi compartments (72) consists almost exclusively of phospholipids (73). Apart from HCV, rabies virus has been the only virus described to contain significant amounts of cholesteryl esters in its envelope even though this virus buds from the plasma membrane (74).

The fatty acid compositions of the major HCV lipids cholesteryl ester and phosphatidylcholine are clearly distinct from the one of Huh7.5 host cells, showing a marked shift toward saturated lipid species, which is a hallmark of viral particles budding from plasma membranes. In contrast, hepatitis C virions resemble (V)LDL particles with respect to their high amounts of incorporated cholesteryl esters, which clearly set them apart from other viruses (51, 61). However, it should be kept in mind that triacylglycerols (TAG), which are well established lipid components of HDL (6 mol %), LDL (10 mol %) and VLDL (60 mol %) (75) could not be determined due to technical difficulties. Given their abundance in lipoproteins, TAGs may constitute a significant proportion of HCV particles, in addition to the lipid classes identified in this study.

Our finding that HCV particles contain ratios of lipid species that are distinct from those of host cell membranes implies that the cellular lipid composition is altered during the course of infection. However, comparative analysis of relative amounts of individual lipid species from naïve and HCV-infected cells did not reveal a difference.[8] Alternatively, HCV may acquire its membrane from specialized intracellular microdomains containing lipids in ratios similar to those of secreted virions. We note that HCV assembly is tightly linked to (cytosolic) lipid droplets and the VLDL synthesis machinery (37). A model has been put forward according to which E1/E2 glycoprotein complexes diffuse from the endoplasmic reticulum membrane bilayer to the budding site of VLDL precursors, thus giving rise to triglyceride-rich lipoproteins carrying viral envelope glycoproteins on their surface (25). This is an attractive model, but because it has been developed by using expression of only E1/E2, it remains to be determined

[7] A. Merz, G. Long, and R. Bartenschlager, unpublished data.

[8] A. Merz, G. Long, B. Brügger, F. Wieland, and R. Bartenschlager, unpublished data.

whether it also applies to assembly of complete HCV particles.

Morphology of HCV Particles—Electron microscopic analyses of affinity-purified Jc1E2^{FLAG} particles revealed heterogeneous structures similar to what has been described earlier (16, 63). E2-labeled particles had an average diameter of 73 ± 18 nm, which is in agreement with previous predictions (9, 15) and observations (9, 16, 54, 63, 76). Particles were predominantly singular (Fig. 6*F*) rather than aggregated with lipoprotein particles as suggested by others (14, 17), arguing against the possibility that our lipid analysis was confounded by nonviral (lipoprotein) particles attached to virions. Importantly, E2-specific immunolabeling or immuno-capture of virus particles was inefficient. Because we used a large panel of poly- and monoclonal antibodies and because some of them potently neutralized infectivity, we argue that the low E2 labeling was not due to poor antibody performance but rather was due to low antigen amounts or epitope accessibility after fixation or both. In support of poor antigen accessibility, capture of FLAG-tagged E2 only with the high avidity FLAG-affinity gel was very efficient. Because the number of E2 proteins per particle is most likely not affected by the tagging, we conclude that either the FLAG beads have an avidity much higher than any of the used E2 antibodies or that the tag is exposed on the surface of the particles and therefore more accessible than the epitope for any of the used E2-specific antibodies. Whatever the reason, we note that similarly low labeling efficiency with an E2-specific antibody (5–20% of density gradient-purified HCV particles) has been reported very recently (76).

Much higher labeling density was obtained for apoE, consistent with the rather high molecule number per particle. Most importantly, two-thirds of all E2 immunoreactive HCV particles could be labeled for apoE in case of the affinity-purified virus preparations. These results show that apoE as well as cholesteryl esters and other lipoprotein-specific lipids are integral components of infectious HCV particles, and they are present either on the particle envelope (*e.g.* apoE) or in its interior (*e.g.* cholesteryl esters).

Because of structural heterogeneity, we could not obtain high enough numbers of particles with consistent morphology to perform three-dimensional reconstructions. Moreover, attempts to study the interior of HCV particles and the composition of the viral envelope by cryo-EM were not successful. Even though we had managed to achieve final Jc1E2^{FLAG} infectivity titers of more than 10^{10} $TCID_{50}$/ml, this concentration was still too low to detect particles within the tiny volumes of the cryo-EM grid holes (~1 fl). In contrast, Gastaminza *et al.* (76) recently reported the first cryo-EM analysis of HCV particles produced in cell culture. These authors used a hyperpermissive Huh7.5 subclone, a cell culture-adapted JFH-1 variant containing a mutation in E2 that increases infectivity and a purification protocol that relies exclusively on density gradient centrifugation rather than immuno-capture. Probably due to higher virus titers in these preparations, HCV particles could be detected that were characterized by an average diameter of ~60 nm and surrounded by a membrane bilayer that was spatially separated from an internal structure. In addition, particles with an average diameter of ~45 nm lacking a membrane bilayer and with high buoyant density were found that might correspond to nonenveloped nucleocapsids (76). Although these data are promising a final proof that the detected structures are indeed infectious, HCV particles is necessary. This will require novel techniques such as immunodetection in combination with cryo-EM.

In conclusion, we developed a rapid and very efficient method to produce large quantities of affinity-purified infectious HCV particles. This method allows the biochemical analysis of the virion with high precision, including its lipidome. The finding that a high proportion of HCV lipids appears to be cholesteryl esters that are incompatible with a regular membrane bilayer raises the challenging question about the membrane organization of the HCV envelope. One possibility is that cholesteryl esters are deposited in-between the envelope bilayer, thus separating the two membrane leaflets giving rise to an "outer and inner monolayer" membrane (68). Whatever the architecture of infectious HCV particles is, understanding lipid imprinting of the virion by the host cell is a fascinating aspect of HCV assembly, and it may provide a starting point to devise novel strategies for efficient antiviral intervention.

Acknowledgments—We are grateful to Ulrike Herian for excellent technical assistance; Charles M. Rice for Huh7.5 cells; Takaji Wakita for provision of the JFH1 clone; John Briggs for helpful EM advice; and to all the following colleagues who kindly provided antibodies essential to carry out this work: H. Tang, T. Baumert, C. M. Rice, A. Patel, and M. Persson. We are very thankful to Claude Antony and the Electron Microscopy Core Facility (EMCF) at EMBL Heidelberg for providing access to their equipment, their expertise, and technical support.

REFERENCES

1. Seeff, L. B. (2002) *Hepatology* **36,** S35–S46
2. Moradpour, D., Penin, F., and Rice, C. M. (2007) *Nat. Rev. Microbiol.* **5,** 453–463
3. Griffin, S. D., Harvey, R., Clarke, D. S., Barclay, W. S., Harris, M., and Rowlands, D. J. (2004) *J. Gen. Virol.* **85,** 451–461
4. Jones, C. T., Murray, C. L., Eastman, D. K., Tassello, J., and Rice, C. M. (2007) *J. Virol.* **81,** 8374–8383
5. Steinmann, E., Penin, F., Kallis, S., Patel, A. H., Bartenschlager, R., and Pietschmann, T. (2007) *PLoS Pathog.* **3,** e103
6. Jirasko, V., Montserret, R., Appel, N., Janvier, A., Eustachi, L., Brohm, C., Steinmann, E., Pietschmann, T., Penin, F., and Bartenschlager, R. (2008) *J. Biol. Chem.* **283,** 28546–28562
7. Bartenschlager, R., Frese, M., and Pietschmann, T. (2004) *Adv. Virus Res.* **63,** 71–180
8. Kato, T., Date, T., Miyamoto, M., Furusaka, A., Tokushige, K., Mizokami, M., and Wakita, T. (2003) *Gastroenterology* **125,** 1808–1817
9. Wakita, T., Pietschmann, T., Kato, T., Date, T., Miyamoto, M., Zhao, Z., Murthy, K., Habermann, A., Kräusslich, H. G., Mizokami, M., Bartenschlager, R., and Liang, T. J. (2005) *Nat. Med.* **11,** 791–796
10. Gottwein, J. M., and Bukh, J. (2008) *Adv. Virus Res.* **71,** 51–133
11. Lindenbach, B. D., Evans, M. J., Syder, A. J., Wölk, B., Tellinghuisen, T. L., Liu, C. C., Maruyama, T., Hynes, R. O., Burton, D. R., McKeating, J. A., and Rice, C. M. (2005) *Science* **309,** 623–626
12. Pietschmann, T., Kaul, A., Koutsoudakis, G., Shavinskaya, A., Kallis, S., Steinmann, E., Abid, K., Negro, F., Dreux, M., Cosset, F. L., and Barten-

schlager, R. (2006) *Proc. Natl. Acad. Sci. U.S.A.* **103,** 7408–7413
13. André, P., Perlemuter, G., Budkowska, A., Bréchot, C., and Lotteau, V. (2005) *Semin. Liver Dis.* **25,** 93–104
14. Nielsen, S. U., Bassendine, M. F., Martin, C., Lowther, D., Purcell, P. J., King, B. J., Neely, D., and Toms, G. L. (2008) *J. Gen. Virol.* **89,** 2507–2517
15. Gastaminza, P., Kapadia, S. B., and Chisari, F. V. (2006) *J. Virol.* **80,** 11074–11081
16. André, P., Komurian-Pradel, F., Deforges, S., Perret, M., Berland, J. L., Sodoyer, M., Pol, S., Bréchot, C., Paranhos-Baccalà, G., and Lotteau, V. (2002) *J. Virol.* **76,** 6919–6928
17. Nielsen, S. U., Bassendine, M. F., Burt, A. D., Martin, C., Pumeechockchai, W., and Toms, G. L. (2006) *J. Virol.* **80,** 2418–2428
18. Lindenbach, B. D., Meuleman, P., Ploss, A., Vanwolleghem, T., Syder, A. J., McKeating, J. A., Lanford, R. E., Feinstone, S. M., Major, M. E., Leroux-Roels, G., and Rice, C. M. (2006) *Proc. Natl. Acad. Sci. U.S.A.* **103,** 3805–3809
19. Gastaminza, P., Cheng, G., Wieland, S., Zhong, J., Liao, W., and Chisari, F. V. (2008) *J. Virol.* **82,** 2120–2129
20. Chang, K. S., Jiang, J., Cai, Z., and Luo, G. (2007) *J. Virol.* **81,** 13783–13793
21. Huang, H., Sun, F., Owen, D. M., Li, W., Chen, Y., Gale, M., Jr., and Ye, J. (2007) *Proc. Natl. Acad. Sci. U.S.A.* **104,** 5848–5853
22. Jiang, J., and Luo, G. (2009) *J. Virol.* **83,** 12680–12691
23. Benga, W. J., Krieger, S. E., Dimitrova, M., Zeisel, M. B., Parnot, M., Lupberger, J., Hildt, E., Luo, G., McLauchlan, J., Baumert, T. F., and Schuster, C. (2010) *Hepatology* **51,** 43–53
24. Nahmias, Y., Goldwasser, J., Casali, M., van Poll, D., Wakita, T., Chung, R. T., and Yarmush, M. L. (2008) *Hepatology* **47,** 1437–1445
25. Icard, V., Diaz, O., Scholtes, C., Perrin-Cocon, L., Ramière, C., Bartenschlager, R., Penin, F., Lotteau, V., and André, P. (2009) *PLoS One* **4,** e4233
26. Owen, D. M., Huang, H., Ye, J., and Gale, M., Jr. (2009) *Virology* **394,** 99–108
27. Maillard, P., Huby, T., Andréo, U., Moreau, M., Chapman, J., and Budkowska, A. (2006) *FASEB J.* **20,** 735–737
28. Voisset, C., Callens, N., Blanchard, E., Op De Beeck, A., Dubuisson, J., and Vu-Dac, N. (2005) *J. Biol. Chem.* **280,** 7793–7799
29. Scarselli, E., Ansuini, H., Cerino, R., Roccasecca, R. M., Acali, S., Filocamo, G., Traboni, C., Nicosia, A., Cortese, R., and Vitelli, A. (2002) *EMBO J.* **21,** 5017–5025
30. Dreux, M., Boson, B., Ricard-Blum, S., Molle, J., Lavillette, D., Bartosch, B., Pécheur, E. I., and Cosset, F. L. (2007) *J. Biol. Chem.* **282,** 32357–32369
31. Meunier, J. C., Engle, R. E., Faulk, K., Zhao, M., Bartosch, B., Alter, H., Emerson, S. U., Cosset, F. L., Purcell, R. H., and Bukh, J. (2005) *Proc. Natl. Acad. Sci. U.S.A.* **102,** 4560–4565
32. Olofsson, S. O., Boström, P., Andersson, L., Rutberg, M., Perman, J., and Borén, J. (2009) *Biochim. Biophys. Acta* **1791,** 448–458
33. Olofsson, S. O., and Borèn, J. (2005) *J. Intern. Med.* **258,** 395–410
34. Hui, D. Y., Innerarity, T. L., and Mahley, R. W. (1981) *J. Biol. Chem.* **256,** 5646–5655
35. Mensenkamp, A. R., Jong, M. C., van Goor, H., van Luyn, M. J., Bloks, V., Havinga, R., Voshol, P. J., Hofker, M. H., van Dijk, K. W., Havekes, L. M., and Kuipers, F. (1999) *J. Biol. Chem.* **274,** 35711–35718
36. Mensenkamp, A. R., Van Luyn, M. J., Havinga, R., Teusink, B., Waterman, I. J., Mann, C. J., Elzinga, B. M., Verkade, H. J., Zammit, V. A., Havekes, L. M., Shoulders, C. C., and Kuipers, F. (2004) *J. Hepatol.* **40,** 599–606
37. Miyanari, Y., Atsuzawa, K., Usuda, N., Watashi, K., Hishiki, T., Zayas, M., Bartenschlager, R., Wakita, T., Hijikata, M., and Shimotohno, K. (2007) *Nat. Cell Biol.* **9,** 1089–1097
38. Koutsoudakis, G., Kaul, A., Steinmann, E., Kallis, S., Lohmann, V., Pietschmann, T., and Bartenschlager, R. (2006) *J. Virol.* **80,** 5308–5320
39. Lohmann, V., Körner, F., Koch, J., Herian, U., Theilmann, L., and Bartenschlager, R. (1999) *Science* **285,** 110–113
40. Kaul, A., Woerz, I., Meuleman, P., Leroux-Roels, G., and Bartenschlager, R. (2007) *J. Virol.* **81,** 13168–13179
41. van den Hoff, M. J., Christoffels, V. M., Labruyère, W. T., Moorman, A. F., and Lamers, W. H. (1995) *Methods Mol. Biol.* **48,** 185–197
42. Spearman, C. (1908) *Br. J. Psychol.* **2,** 227–242
43. Kärber, G. (1931) *Arch. für ex. Path. Pharm.* **162,** 480–487
44. Jones, C. T., Catanese, M. T., Law, L. M., Khetani, S. R., Syder, A. J., Ploss, A., Oh, T. S., Schoggins, J. W., MacDonald, M. R., Bhatia, S. N., and Rice, C. M. (2010) *Nat. Biotechnol.* **28,** 167–171
45. Owsianka, A., Clayton, R. F., Loomis-Price, L. D., McKeating, J. A., and Patel, A. H. (2001) *J. Gen. Virol.* **82,** 1877–1883
46. Johansson, D. X., Voisset, C., Tarr, A. W., Aung, M., Ball, J. K., Dubuisson, J., and Persson, M. A. (2007) *Proc. Natl. Acad. Sci. U.S.A.* **104,** 16269–16274
47. Bligh, E. G., and Dyer, W. J. (1959) *Can. J. Biochem. Physiol.* **37,** 911–917
48. Brügger, B., Erben, G., Sandhoff, R., Wieland, F. T., and Lehmann, W. D. (1997) *Proc. Natl. Acad. Sci. U.S.A.* **94,** 2339–2344
49. Brügger, B., Graham, C., Leibrecht, I., Mombelli, E., Jen, A., Wieland, F., and Morris, R. (2004) *J. Biol. Chem.* **279,** 7530–7536
50. Brügger, B., Sandhoff, R., Wegehingel, S., Gorgas, K., Malsam, J., Helms, J. B., Lehmann, W. D., Nickel, W., and Wieland, F. T. (2000) *J. Cell Biol.* **151,** 507–518
51. Brügger, B., Glass, B., Haberkant, P., Leibrecht, I., Wieland, F. T., and Kräusslich, H. G. (2006) *Proc. Natl. Acad. Sci. U.S.A.* **103,** 2641–2646
52. Liebisch, G., Binder, M., Schifferer, R., Langmann, T., Schulz, B., and Schmitz, G. (2006) *Biochim. Biophys. Acta* **1761,** 121–128
53. Koivusalo, M., Haimi, P., Heikinheimo, L., Kostiainen, R., and Somerharju, P. (2001) *J. Lipid Res.* **42,** 663–672
54. Yu, X., Qiao, M., Atanasov, I., Hu, Z., Kato, T., Liang, T. J., and Zhou, Z. H. (2007) *Virology* **367,** 126–134
55. Vieyres, G., Thomas, X., Descamps, V., Duverlie, G., Patel, A. H., and Dubuisson, J. (2010) *J. Virol.* **84,** 10159–10168
56. Evans, M. J., Rice, C. M., and Goff, S. P. (2004) *Proc. Natl. Acad. Sci. U.S.A.* **101,** 13038–13043
57. Kaul, A., Stauffer, S., Berger, C., Pertel, T., Schmitt, J., Kallis, S., Zayas, M., Lopez, M. Z., Lohmann, V., Luban, J., and Bartenschlager, R. (2009) *PLoS Pathog.* **5,** e1000546
58. Ciesek, S., Steinmann, E., Wedemeyer, H., Manns, M. P., Neyts, J., Tautz, N., Madan, V., Bartenschlager, R., von Hahn, T., and Pietschmann, T. (2009) *Hepatology* **50,** 1638–1645
59. Yang, F., Robotham, J. M., Nelson, H. B., Irsigler, A., Kenworthy, R., and Tang, H. (2008) *J. Virol.* **82,** 5269–5278
60. Pietschmann, T., Lohmann, V., Kaul, A., Krieger, N., Rinck, G., Rutter, G., Strand, D., and Bartenschlager, R. (2002) *J. Virol.* **76,** 4008–4021
61. Kalvodova, L., Sampaio, J. L., Cordo, S., Ejsing, C. S., Shevchenko, A., and Simons, K. (2009) *J. Virol.* **83,** 7996–8003
62. Wiesner, P., Leidl, K., Boettcher, A., Schmitz, G., and Liebisch, G. (2009) *J. Lipid Res.* **50,** 574–585
63. Parent, R., Qu, X., Petit, M. A., and Beretta, L. (2009) *Hepatology* **49,** 1798–1809
64. Maillard, P., Krawczynski, K., Nitkiewicz, J., Bronnert, C., Sidorkiewicz, M., Gounon, P., Dubuisson, J., Faure, G., Crainic, R., and Budkowska, A. (2001) *J. Virol.* **75,** 8240–8250
65. Masciopinto, F., Giovani, C., Campagnoli, S., Galli-Stampino, L., Colombatto, P., Brunetto, M., Yen, T. S., Houghton, M., Pileri, P., and Abrignani, S. (2004) *Eur. J. Immunol.* **34,** 2834–2842
66. Takahashi, H., Akazawa, D., Kato, T., Date, T., Shirakura, M., Nakamura, N., Mochizuki, H., Tanaka-Kaneko, K., Sata, T., Tanaka, Y., Mizokami, M., Suzuki, T., and Wakita, T. (2010) *Biochem. Biophys. Res. Commun.* **395,** 565–571
67. Podevin, P., Carpentier, A., Pène, V., Aoudjehane, L., Carrière, M., Zaïdi, S., Hernandez, C., Calle, V., Méritet, J. F., Scatton, O., Dreux, M., Cosset, F. L., Wakita, T., Bartenschlager, R., Demignot, S., Conti, F., Rosenberg, A. R., and Calmus, Y. (2010) *Gastroenterology* **139,** 1355–1364
68. Bartenschlager, R., Penin, F., Lohmann, V., and André, P. (2011) *Trends Microbiol.,* in press
69. Felmlee, D. J., Sheridan, D. A., Bridge, S. H., Nielsen, S. U., Milne, R. W., Packard, C. J., Caslake, M. J., McLauchlan, J., Toms, G. L., Neely, R. D., and Bassendine, M. F. (2010) *Gastroenterology* **139,** 1774–1783

70. Ciesek, S., Friesland, M., Steinmann, J., Becker, B., Wedemeyer, H., Manns, M. P., Steinmann, J., Pietschmann, T., and Steinmann, E. (2010) *J. Infect. Dis.* **201,** 1859–1866
71. Aizaki, H., Morikawa, K., Fukasawa, M., Hara, H., Inoue, Y., Tani, H., Saito, K., Nishijima, M., Hanada, K., Matsuura, Y., Lai, M. M., Miyamura, T., Wakita, T., and Suzuki, T. (2008) *J. Virol.* **82,** 5715–5724
72. Bruss, V. (2004) *Virus Res.* **106,** 199–209
73. Satoh, O., Umeda, M., Imai, H., Tunoo, H., and Inoue, K. (1990) *J. Lipid Res.* **31,** 1293–1300
74. Schlesinger, H. R., Wells, H. J., and Hummeler, K. (1973) *J. Virol.* **12,** 1028–1030
75. Murphy, D. J. (2001) *Prog. Lipid Res.* **40,** 325–438
76. Gastaminza, P., Dryden, K. A., Boyd, B., Wood, M. R., Law, M., Yeager, M., and Chisari, F. V. (2010) *J. Virol.* **84,** 10999–11009